Carbonation-induced corrosion: investigation of the corrosion onset

Andres Belda Revert[1], Klaartje De Weerdt[1], Karla Hornbostel[2], Mette Rica Geiker[1]

[1]*Norwegian University of Science and Technology. Department of Structural Engineering.* andres.b.revert@ntnu.no

[2]*Norwegian Public Roads Administration (Statens vegvesen), Trondheim, Norway*

Abstract

There are different views in the literature on the relationship between the location of the carbonation front and the onset of reinforcement corrosion. Theoretically, corrosion starts when the carbonation front reaches the reinforcement, but some authors have observed an apparent earlier start of corrosion. In the present study, mortar samples with and without reinforcement were exposed up to 22 weeks to 20 °C, 60% RH and 1.5% CO_2. The state of the reinforcement was monitored by potential measurements of potential. The carbonation of the bulk and the mortar-steel interface was detected by spraying a pH indicator on a freshly split or cut surface. Good agreement was found between low potential values (compared to reinforcement in the passive state) and the carbonation of the mortar-steel interface. A difference in the spatial variation of the carbonation depth was observed between plain and reinforced samples. The differences found in the literature between the location of the carbonation front and the corrosion onset can probably be explained by the spatial variation of the carbonation depth in the vicinity of the reinforcement.

Keywords:

Carbonation, Corrosion onset, pH indicator, Corrosion potential, Petrographic analysis

Abbreviations:

CO_2: carbon dioxide concentration in the air (volume)

D_{max}: maximum aggregate size

FA: fly ash

GGBFS: ground-granulated blast-furnace slag

L: limestone

OCP: open-circuit potential

pH: pH indicator

RH: relative humidity

SCE: saturated calomel reference electrode

t: time

T: temperature

w/b: water-to-binder ratio

w_x: width of the carbonation front

$x_{c,i}$: carbonation depth measurement "i"

δ_x: spatial variation of the carbonation depth

Ø: reinforcement diameter

1. Introduction

Corrosion is one of the major causes of deterioration in reinforced concrete structures [1]. Chloride ingress and carbonation are the most common causes of initiation of reinforcement corrosion. Reinforcement embedded in concrete is prevented from corrosion by a thin layer of iron oxides, which is stable in the high-alkaline environment of sound concrete [2]. Upon carbonation, the pH of the pore solution is reduced to values below 7 [3]. The oxide layer is no longer stable in such a low pH and reinforcement embedded in carbonated concrete can corrode depending on the exposure. Differences are found in the literature on the location of the carbonation front and the onset of the reinforcement corrosion. Some authors have observed that reinforcement corrosion can start before the carbonation depth compares to the concrete cover. Table 1 presents a summary of published experimental investigations on carbonation-induced corrosion onset.

Table 1: Summary of the experimental investigations on carbonation-induced corrosion onset

Authors		Parrot, J. [4], [5]	Yoon et al. [6]	Hussain et al. [7], [8]
Materials	Type	Concrete	Concrete	Concrete
	SCMs	FA, GGBFS, L	-	-
	w/b	0.35, 0.47, 0.59, 0.71, 0.83	0.45, 0.5, 0.55	0.45
Geometry	Samples [mm]	Cubes, 100	Prims, length 200	Prims, 200x100x100
	Cover [mm]	4, 8, 12 and 20	12	13
	D_{max} [mm]	10	25	20
	Ø [mm]	6.4	8	13
Curing	T [°C]	not reported	20	20
	Moisture conditions	Wet cured	Wet cured	Sealed
	t [days]	1, 3, 28	28	28
Exposure	T [°C]	Indoors	20	20
	RH [%]	45–58%	65	55
	CO_2 [%]	0.04%, outdoors, sheltered, outdoors, exposed	3, 5, 10	10
Characterization	Carbonation	pH in plain samples	pH in plain samples	pH in plain samples
	Corrosion onset	Gravimetric analysis	Gravimetric analysis, LPR	Corrosion potential
	Criteria for corrosion onset	Weight loss [not reported]	Weight loss 0.2–0.5 g	Potential drop ≈ 200 mV

FA: fly ash, GGBFS: ground granulated-blast furnace slag, L: limestone, D_{max}: maximum aggregate size, Ø: reinforcement diameter, pH: pH indicator

Parrott detected corrosion when the difference between the average carbonation depth in plain concrete and the concrete cover (in reinforced samples), the "unneutralized remainder", was 10–15 mm, i.e. he observed corrosion before the apparent carbonation front reached the reinforcement [4], [5]. He determined ongoing corrosion by gravimetric analysis of the reinforcement, and from the unneutralized remainder from the carbonation depth measurements in plain samples. For further description of materials and exposure conditions, see Table 1. Carbonation development in the plain samples and corrosion in the reinforced samples were measured after 6, 18 and 48 months of exposure.

Yoon et al. also compared the corrosion onset in reinforced samples with carbonation depth measurements in plain samples. They found that corrosion started before the apparent carbonation front reached the reinforcement, but as long as the unneutralized remainder was more than 5–10 mm in thickness the risk of carbonation-induced corrosion was low [6]. This is in agreement with the findings by Parrott [4], [5], although the unneutralized remainder determined is lower. For further description of materials and exposure conditions, see Table 1. Carbonation development was monitored in the plain samples and the corrosion rate in the reinforced samples using linear polarization resistance and gravimetric analysis at the end of the exposure.

In agreement with the above observations, Hussain et al. found that corrosion started when the carbonation depth in plain samples was 80% of the concrete cover [8]. For further description of materials and exposure conditions, see Table 1. The corrosion potential was monitored during the exposure and the corrosion rate was estimated from gravimetric analysis of the reinforcement after exposure. Corrosion onset was identified by a potential drop of 200 mV.

The above observations are also reflected in JSCE Guidelines, which state that corrosion starts before the carbonation front reaches the reinforcement: *"It has been learned from laboratory tests and investigations on actual structures that the corrosion of steel may begin before the*

carbonation depth actually exceed(s) the cover thickness" [9]. According to the JSCE, to avoid corrosion onset the unneutralized remainder should be at least 10 mm, and as much as 25 mm if chlorides are present. No references are given to support these statements.

In this study, we investigated three possible hypotheses that could explain the apparent early onset of carbonation-induced reinforcement corrosion:

1. Width of carbonation front (w_x). When detecting carbonation, there will be a volume range where the investigated property changes from sound to carbonated concrete. The detected width of this carbonation front depends on the characterisation method used [10]. A large carbonation front width could lead to conditions for corrosion onset before carbonation can be detected at the level of the reinforcement.
2. Spatial variation of carbonation depth:
    2.1. Spatial variation in plain samples (δ_x). The spatial variation in the carbonation depth measured in plain samples could induce corrosion on parts of the reinforcement before the average carbonation depth reaches the level of the reinforcement.
    2.2. Spatial variation in reinforced samples (δ_x). Differences in microstructure between plain and reinforced samples could induce differences in the spatial variation of the carbonation depth and faster carbonation in the vicinity of the reinforcement.

Figure 1 illustrates the nomenclature used. Moreover, when we refer to the data from the literature, all the authors detected the carbonation in plain samples, so the term "apparent" carbonation front is used.

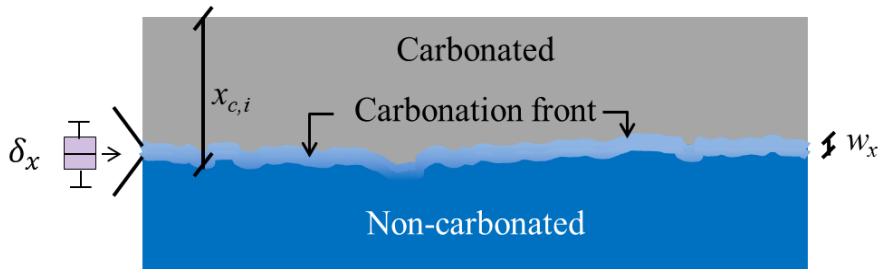

Figure 1: Nomenclature used: δ_x: spatial variation of the carbonation depth, $x_{c,i}$: carbonation depth measurement "i", w_x: width of the carbonation front. The sketch illustrates carbonation detected using a pH indicator, adapted from previous work [10].

Mortar samples varying in size and reinforcement position were prepared using 3 different compaction methods. The samples were sealed, cured for 2 weeks, and exposed to accelerated carbonation for up to 22 weeks. The state of the embedded steel was monitored by potential measurements. The carbonation of the bulk and the mortar-steel interface was studied by spraying a pH indicator on a freshly split or cut surface. In addition, thin sections were investigated using optical microscopy. We found that the embedded steel affects the spatial variation of the carbonation depth, possibly due to differences in microstructure between plain and reinforced samples. These differences cannot be attributed to the specific materials or the exposure; similar observations were reported in a field assessment [11]. Based on these observations, monitoring carbonation development in plain samples and assuming similar carbonation development in reinforced samples might give non-conservative prediction of the corrosion onset.

2. Experimental

A set of plain and reinforced mortar samples with different geometries were prepared using various compaction methods: jolted (J), vibrated (V) and tapped (T). Table 2 summarizes the experimental matrix.

Table 2: Summary of samples and measurements. Reinforced (A, B and C) and plain (A' and C').

Samples				Property investigated				
				OCP		Carbonation		Micro-structure
Id.	Size [mm]	Compaction method	No.	Bars	Duration [weeks]	Bulk	Mortar-steel interface	
A	40 x40 x160	Jolted (J)	2	1	20	x	-	-
		Vibrated (V)	1	1	20	x	-	-
		Tapped (T)	1	1	20	x	-	-
A'	40 x40 x160	Jolted (J)	1	-	-	x	-	-
		Vibrated (V)	1	-	-	x	-	-
		Tapped (T)	1	-	-	x	-	-
B	120 x40 x160	Vibrated (V)	1	3	20	-	-	-
		Tapped (T)	1	3	20	-	-	-
C	120 x80 x160	Vibrated (V)	1	8	10	x	x	-
		Tapped (T)	1	8	10	x	x	x
C'	120 x80 x160	Vibrated (V)	1	-	-	x	-	-
		Tapped (T)	1	-	-	x	-	-

2.1. Geometry

Reinforced (A, B and C) and plain (A' and C') mortar samples were prepared. The reinforced samples contained ribbed carbon steel bars (Ø 6 mm) embedded in different positions, but always with a 10 mm cover, see Figure 2. Type A samples contained only one reinforcement bar, type B three bars, and type C eight bars (for labelling of the bars, cf. Figure 2). In addition, one stainless steel bar was embedded in the middle of the C samples, cf. Figure 2. In the following sections, the samples are labelled as follows: <sample type>-<compaction method>-<bar position>, e.g. 120x80x160 mm tapped samples with reinforcement in position 1 are labelled: C-T-1.

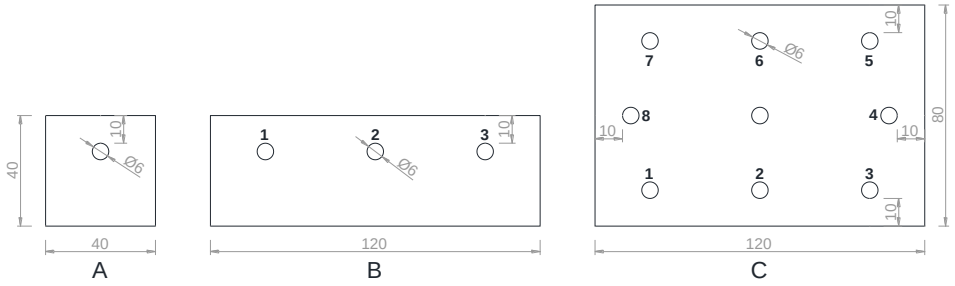

Figure 2: Reinforced mortar samples [mm]. A' and C' plain mortar samples have the same geometry as A and C. Numbers refer to the position of steel bars. The mortar was poured from the top.

2.2. Mortar composition and reinforcement

The mortar samples contained Portland-fly ash cement (CEM II/B-V in accordance with EN-197-1 [12]) supplied by NORCEM AS and standard sand in accordance with EN 196-1 [13] (D_{max} 2 mm). Filtered tap water was used for the mixing. The XRF analysis of the cement given by NORCEM AS is: 29.5% SiO_2, 10.8% Al_2O_3, 4.5% Fe_2O_3, 44.6% CaO, 2% MgO, 3.2% SO_3, 0.4% P_2O_5, 1.1% K_2O, 0.5% Na_2O, and 0.03 chlorine.

The recipe was based on EN 196-1 [13], but the cement and water content was adjusted to obtain w/b 0.55, keeping the volumetric paste-sand ratio constant. Two batches (each approximately 12 litres) were required to cast all the samples. The following amount of each component was required per batch: 4355 g of cement, 2395 g of water and 13,500 g of sand. The mixing steps were as defined in EN 196-1 [13], except that the mixer was used with a constant mixing speed. Water and binder were placed in the mixing bowl and the mixer was immediately started. After 30 seconds of mixing, sand was added steadily over the next 30 seconds, and the mortar was mixed for 30 more seconds once all the sand had been added. The mixing was stopped for 90 seconds while the mortar adhering to the wall and bottom of the bowl was detached and moved to the middle of the bowl. Finally, the mixing was continued for another 60 seconds. Ribbed carbon steel bars 6 mm in diameter (B500NC in accordance with NS 3576 [14]) were used as reinforcement, and an additional AISI 2205 6 mm bar was embedded in the middle of the type C samples for use as a pseudo-reference electrode. The reinforcement was cut into 160 mm pieces and both ends were polished. The steel was cleaned in HCl containing urotropine (HCl 1:1 + 3g/l urotropine), placed in an ultrasonic bath for 5 minutes, rinsed with distilled water, and dried using a hairdryer. Finally, 30 mm of both ends of each bar were coated with beeswax by dipping the reinforcement into the melted wax twice. The reinforcement pieces were kept in a desiccator including a drying agent (silica gel), until they were embedded in mortar.

2.3. Preparation of the samples

Three compaction methods were used to prepare the samples: jolting, vibrating table, and tapping. Jolting is the standard compaction method for mortar samples according to EN 196-1 [13], in which the moulds are filled in two layers, applying sixty jolts per layer. For the vibrating table compaction, 20 mm layers were compacted by applying 5 seconds of vibration, frequency 50 Hz and vertical amplitude 0.65 mm, to each layer. The mould was firmly held against the vibrating table during compaction. The vibration time was selected on the basis of the cessation of air bubbles and limited bleeding. For the tapping compaction, a 6 mm diameter, smooth, straight, stainless steel rod with rounded ends was used. 20 mm layers were tapped compact by applying 30 strokes per layer uniformly distributed over the cross section of the mould. The first layer was compacted without tapping the bottom of the mould and the subsequent layers were compacted avoiding penetration of the previous layers. At the end, the sides of the mould were gently tapped with the steel rod until large air bubbles ceased to appear.

The samples were kept in the moulds covered with plastic for one day after casting at room temperature (approx. 20 °C). Then they were demoulded, wrapped in plastic, and stored at 20 °C for 13 days.

2.4. Exposure

After the 14 curing days, the samples were exposed to 20 °C, 60 ± 2% RH, and 1.5 ± 0.1% CO_2 for up to 22 weeks in climate cabinets with forced ventilation, which were set up to ensure homogeneous exposure conditions for the samples.

2.5. Methods

2.5.1. Open circuit potential (OCP)

The open circuit potential (OCP) of the embedded steel was monitored using an external saturated calomel reference electrode (SCE) and a high impedance voltmeter (Fluke 76, input impedance 10 MΩ). Ultrasound gel was applied on the mortar surface to provide electrical contact. The OCP was monitored twice a week.

2.5.2. Carbonation characterization

Carbonation was detected by spraying a thymolphthalein solution on either a freshly split or a freshly dry-cut sample. Pictures were taken using an Olympus E-630 camera attached to a set-up with fixed lighting conditions. The thymolphthalein solution was prepared by dissolving 1 gram of the indicator (powder, grade "ACS, Reag. Ph Eur" (VWR)) in a mix of 30 ml of deionized water and 70 ml of ethanol. The colour change of thymolphthalein occurs in the pH range of 9 to 10.5. Above this range, an intense bluish colour is observed while, below it, thymolphthalein becomes colourless. Phenolphthalein is the pH indicator recommended for detecting carbonation according to EN 13295 [15], but it has been classified as carcinogenic [16]. We have previously tested thymolphthalein on the same materials and exposure, and observed similar carbonation depths to those found with phenolphthalein [10].

The distribution of the carbonation depth was determined by image analysis using a colour threshold principle. First, the pictures were scaled, then the sample area and the non-carbonated area were determined, and finally the carbonation depths were measured. When taking measurements, we avoided the corners (due to the ingress from two directions).

The carbonation of the mortar-steel interface was investigated by splitting reinforced samples longitudinally and spraying the imprint of the reinforcement bar (the mortar-steel interface) with thymolphthalein. To quantify the carbonated fraction of the mortar-steel interface, the colour threshold of the pictures was manually adjusted to differentiate more clearly between the carbonated and non-carbonated areas. Next, the interface was discretized in a 1x1 mm grid and the state of each cell was assessed (carbonated or non-carbonated). A geometric factor was applied to take into account the circular shape of the reinforcement. The mortar-steel interface of the reinforcement bars in some of the vibrated samples could not be investigated, because the samples broke into small pieces when split longitudinally.

2.5.3. Petrographic analysis of thin sections

Thin sections were prepared at the Danish Technological Institute in accordance with Nordtest [17] for a general investigation of the microstructure. The samples were impregnated with an epoxy resin containing fluorescent dye, mounted on a glass plate, ground to a thickness of 20 µm, and then covered with a second glass plate. The thin sections prepared included reinforcement located in three different positions (bottom, middle and top) from sample C-T. The thin sections were prepared after 22 weeks of exposure (after corrosion onset). The thin sections were investigated with an optical microscope Nikon Eclipse LV 100 POL using transmitted, crossed polarized and fluorescent light.

3. Results

3.1. Open circuit potential (OCP)

Figure 3 presents the OCP measurements in the A and B samples over 20 weeks. Figure 4 presents a summary of the OCP measurements in the C samples over the first 10 weeks of exposure. The mortar-steel interface of the C samples was investigated after 10 weeks of exposure.

3.2. Carbonation depth

Figure 5 presents the carbonation investigation of the A' samples. The carbonation front presented a trapezoidal shape in the jolted samples, indicating separation in these samples. The other two compaction methods seem to have caused less segregation, leaving the top and lateral sides comparable. The impact of an air bubble is observed in the tapped sample (Figure 5, right). Figure 6 shows the carbonation front in the C'-T and C-T samples after 10 and 22 weeks of exposure. Similar trends were observed in the vibrated samples, which are not shown here. Figure 7 presents the histograms of the carbonation depth measurements taken in the plain C'-T after 10 and 22 weeks of exposure. The data set includes the measurements from the top and lateral sides. Figure 8 and Figure 9 present the carbonation of the mortar-steel interface for the reinforced C-T and C-V samples after 10 weeks of exposure. Note that the data from the vibrated samples is limited due to problems with the sampling.

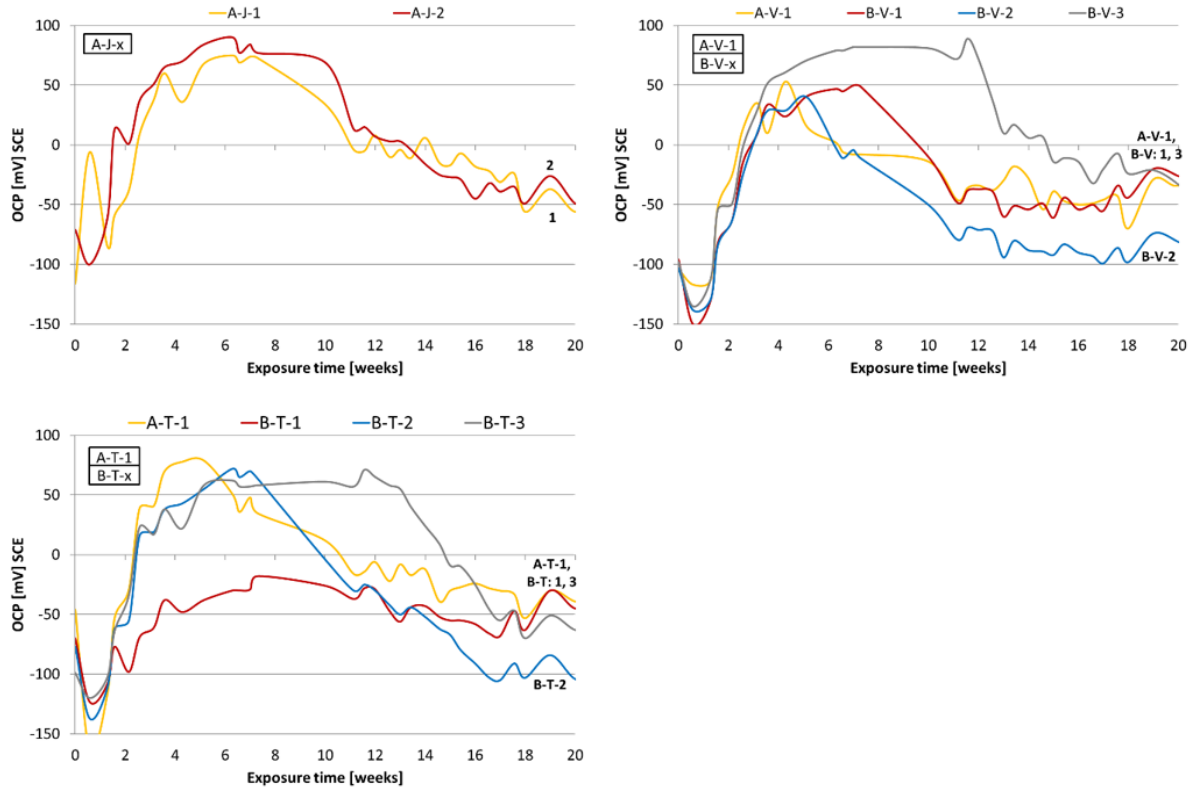

Figure 3: OCP of jolted (J) , vibrated (V) and tapped (T) 40x40x160 (A) and 120x40x160 mm (B) samples over the first 20 weeks of exposure at 20 °C, 60% RH, and 1.5% CO_2.

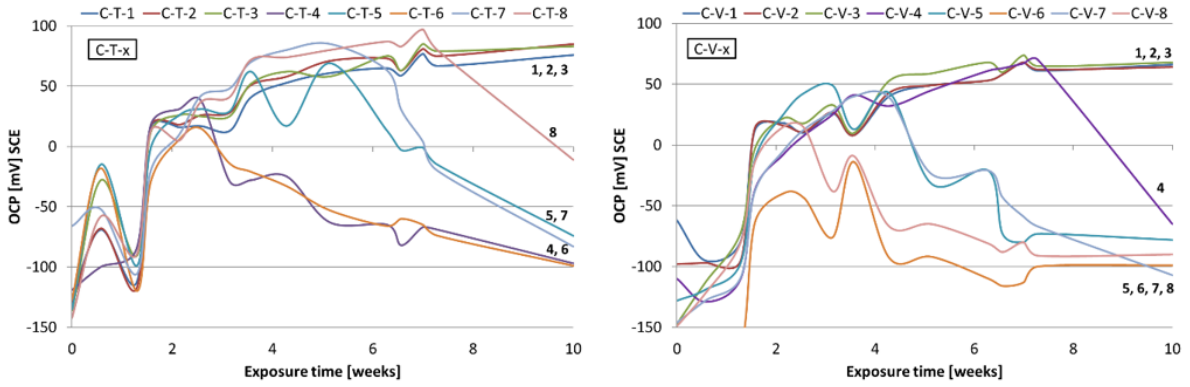

Figure 4: OCP of tapped (T) and vibrated (V) 120x80x160 mm (C) samples over 10 weeks of exposure at 20 °C, 60% RH, and 1.5% CO_2.

Figure 5: Carbonation detection in the plain A' (40x40x160 mm) mortar samples. From left to right: cross sections of A'-J, A'-V and A'-T. The samples were sprayed with thymolphthalein after 8 weeks of exposure.

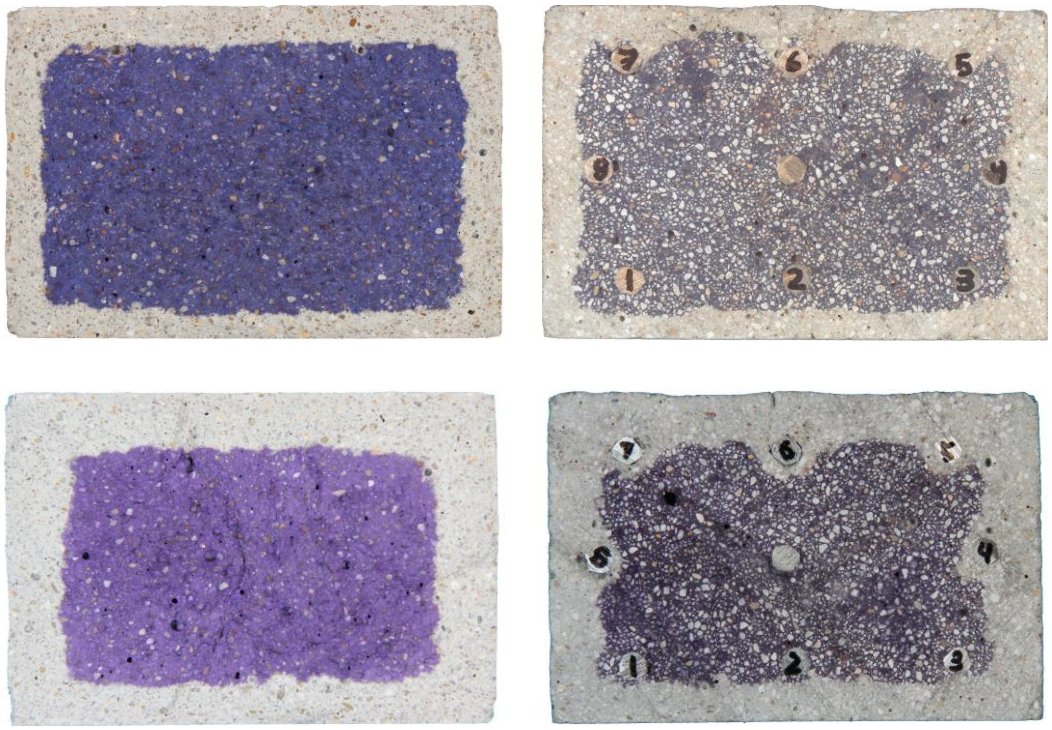

Figure 6: Carbonation detection in C'-T and C-T samples (120x80x160 mm). Cross sections sprayed with thymolphthalein after 10 weeks (top) and 22 weeks (bottom) of exposure.

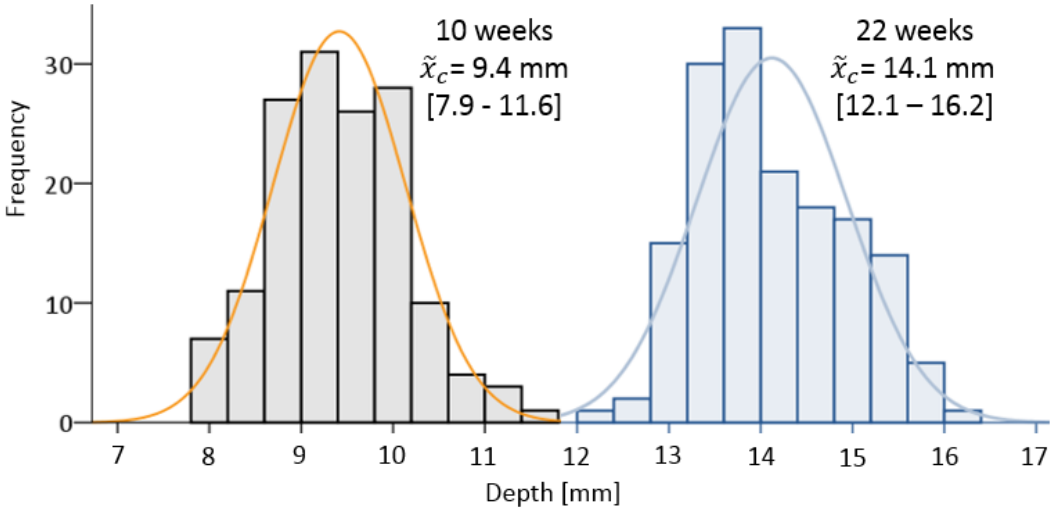

Figure 7: Carbonation depth histograms of the plain C'-T mortar sample after 10 and 22 weeks of exposure, giving average and range. The line shows the normal distribution curve.

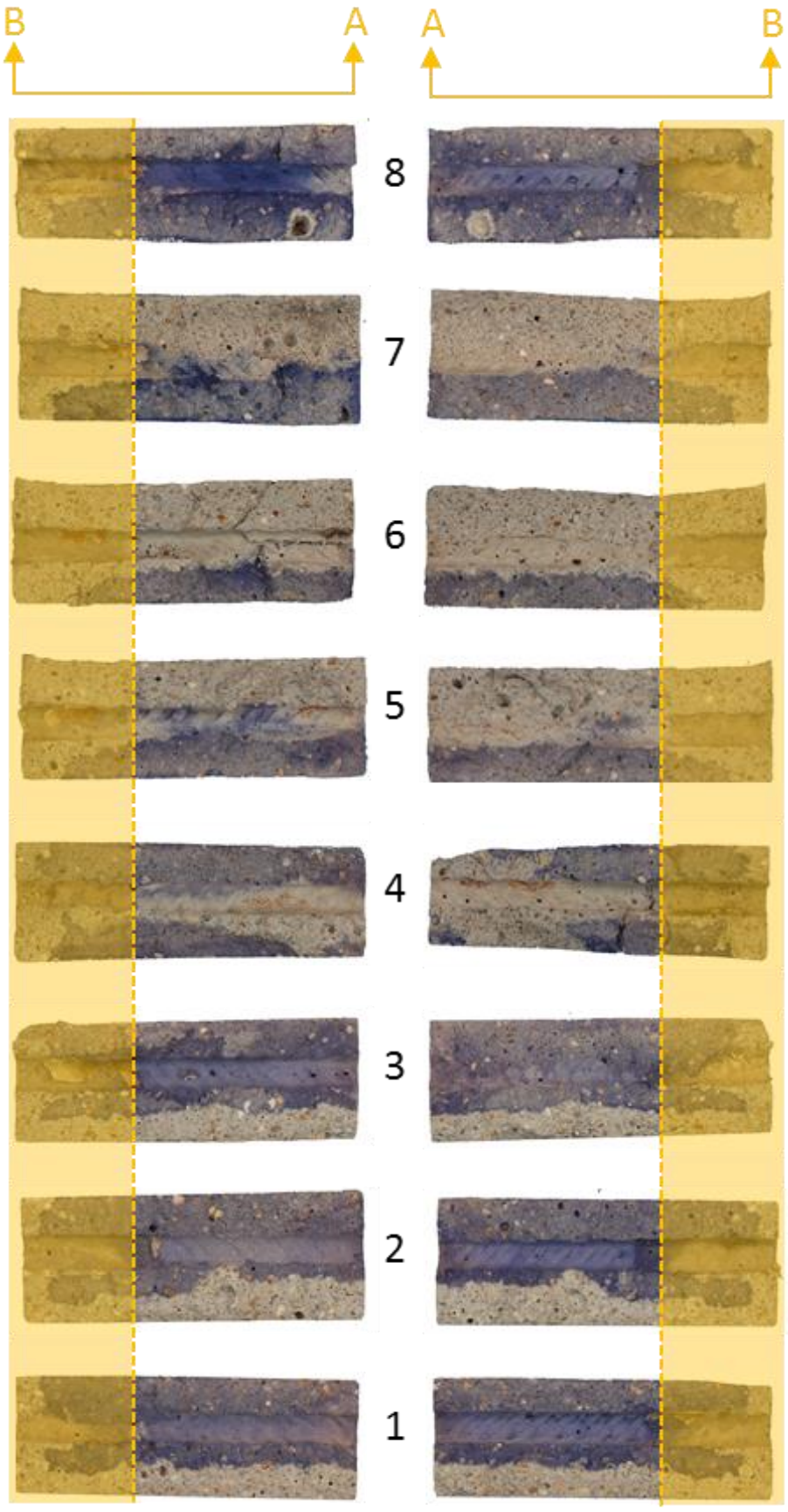

Figure 8: Carbonation investigation of the mortar-steel interface of the C-T sample after 10 weeks of exposure. The shaded areas represent the length of the reinforcement which was coated with beeswax.

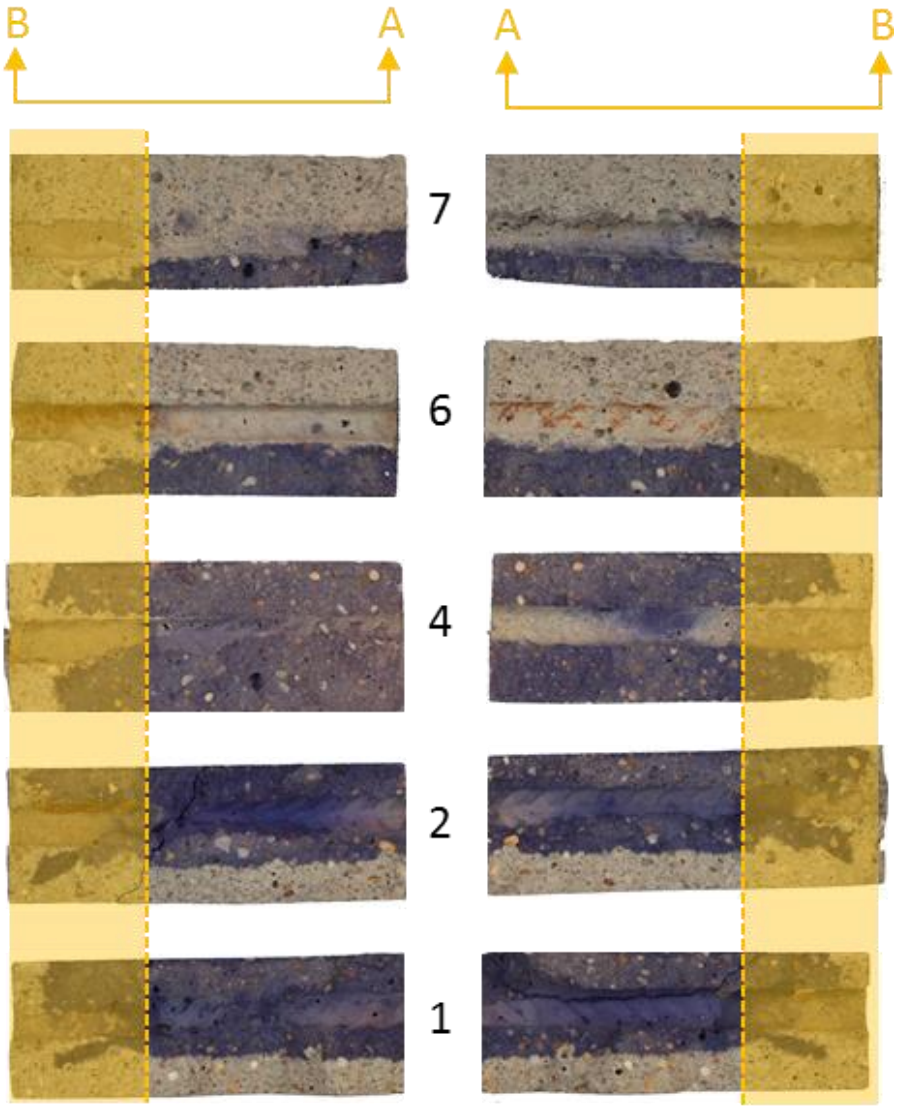

Figure 9: Carbonation investigation of the mortar-steel interface of the C-V sample after 10 weeks of exposure. The shaded areas represent the length of the reinforcement which was coated with beeswax.

3.3. Petrographic analysis of thin sections

Figure 10 presents micrographs taken by Ulla Hjorth Jakobsen (DTI) and sketches of microcracking observed. Photographs using fluorescent lighting were taken close to the reinforcement in the top, middle and bottom positions. A radial crack pattern was observed in the vicinity of the reinforcement in the top and middle positions, while fewer cracks and a different pattern were observed in the vicinity of the bottom reinforcement. According to Ulla Hjorth Jakobsen, all the cracks observed were formed during the plastic stage and were smaller than 10 µm. If we compare the greenish colours of the micrographs, a small difference in

porosity can be observed between the thin sections from the bottom and the top and middle positions. However, it was not possible to quantify this difference.

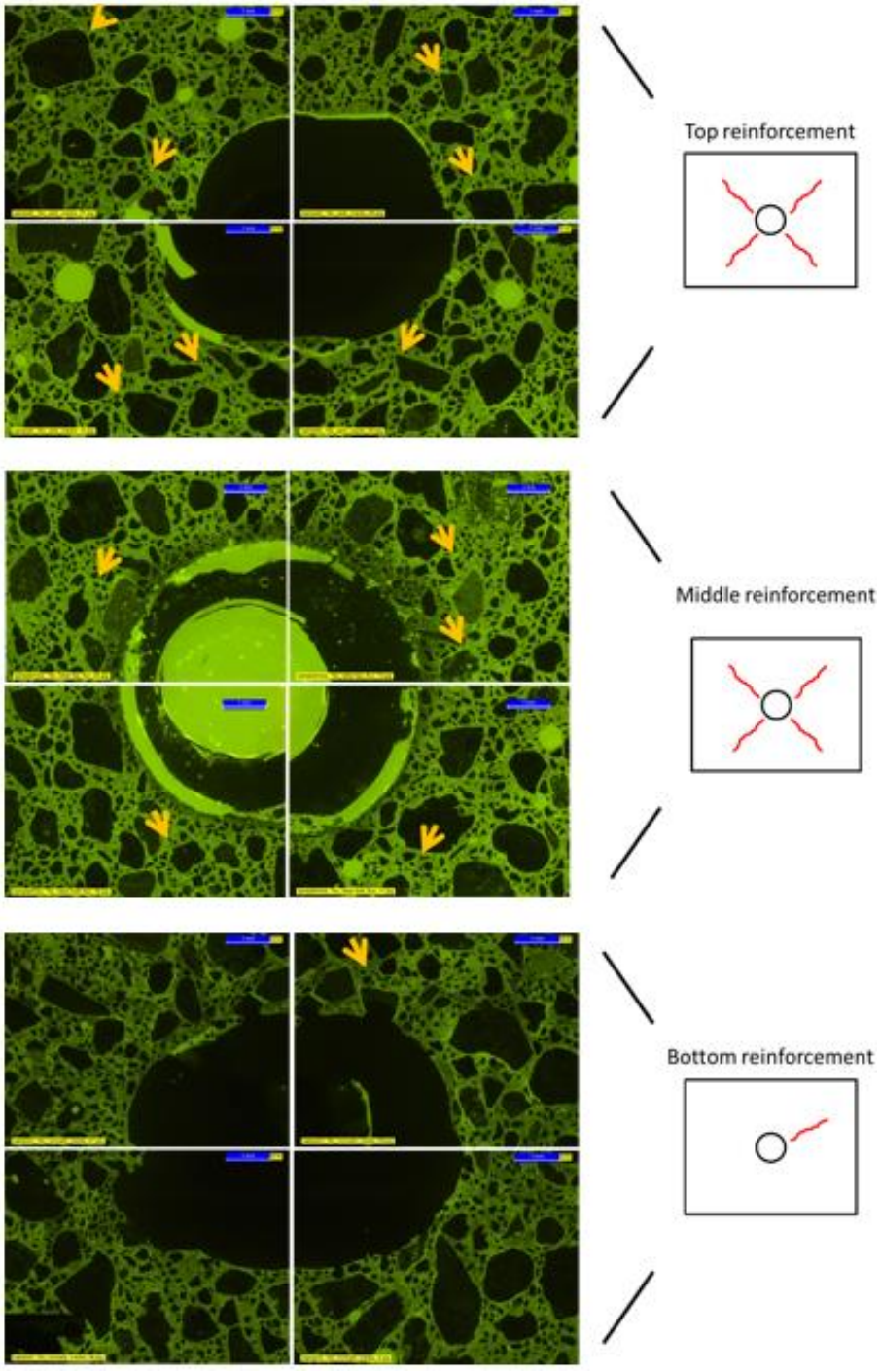

Figure 10: Micrographs taken in fluorescent light using an optical microscope with magnification x16 (width of each micrograph 6.5 mm) on the C–T sample after 22 weeks of exposure. Arrows indicate the cracks observed. Crack patterns observed in the top, middle and bottom reinforced samples are included in the sketches on the right.

4. Discussion

4.1. Relationship between carbonation of the mortar-steel interface and the OCP

The pictures shown in Figure 8 and Figure 9 were used to quantify the carbonated fraction of the mortar-steel interface. In Figure 11, the carbonated fraction of the interface is plotted against the OCP for each reinforcement bar at the time the samples were split (after 10 weeks of exposure). During the carbonation of the mortar-steel interface, there seems to be a gradual change towards more negative OCP values. Similar OCP trends were observed during carbonation in all the samples regardless the compaction method. Although the data is limited, we found that the carbonated fraction of the mortar-steel interface correlates with the OCP measured. For steel embedded in non-carbonated mortar, OCP in the range of +60 to +90 mV vs. SCE was measured, whereas when the carbonated fraction of the mortar-steel interface exceeded 75% the values gathered around -70 to -110 mV vs. SCE. Overall, we observed that a drop of approx. 140–200 mV in the OCP indicated the complete carbonation of the mortar-steel interface. The OCP remained within the same range after the onset of corrosion, see Figure 3. On this basis, we conclude that the OCP drop was due to the carbonation of the mortar-steel interface rather than other factors, e.g. moisture changes.

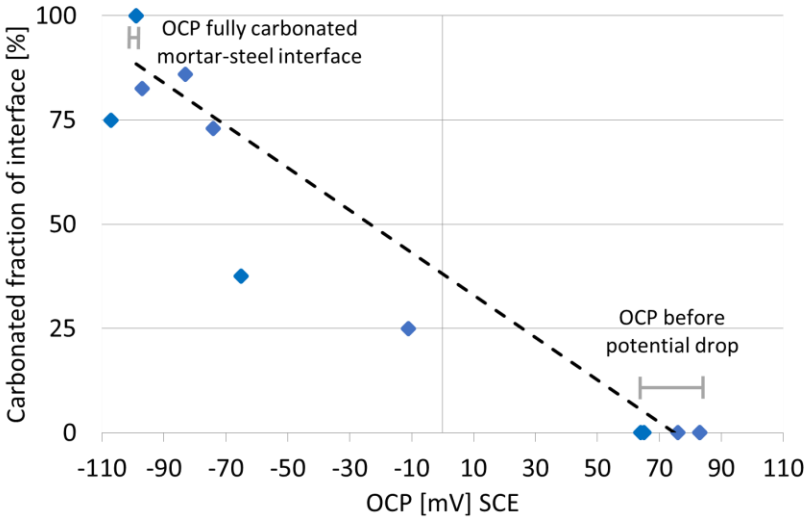

Figure 11: Relationship between the carbonated fraction of the mortar-steel interface and the OCP measured in the C samples. 100% means complete carbonation of the mortar-steel interface and 0% means no carbonation.

RILEM TC-235 CTC defines the onset of chloride-induced corrosion as follows: *"significant drop of the measured potential, and the corrosion activity is defined as being stable when the potential has dropped and remained at a potential at least 150 mV lower than the passive level for more than 7 days"* [18]. The literature reports a similar potential drop for carbonation-induced corrosion [7], [8], which is in agreement with the present study. However, for carbonation-induced corrosion, the time required for stable OCP indicating corrosion seems to be longer. In the present study, a gradual change in OCP towards more negative values was observed. The change in potential took from 4 to 10 weeks depending on the sample, see Figure 3. We attribute the gradual change in OCP to the steady carbonation of the mortar-steel interface, as shown in Figure 11. In contrast to what is typically seen for chloride-induced corrosion, there was no indication of re-passivation of the steel embedded in the carbonated mortar within the test period.

4.2. Width of the carbonation front

When detecting carbonation using a pH indicator, the pH threshold of the indicator should be taken into account. In a previous investigation, we compared a set of pH indicators, including phenolphthalein (pH 8.2–9.8) and thymolphthalein (pH 9–10.5) among other indicators [19]. Comparable carbonation depths were measured and all the indicators illustrated a sharp drop in pH and a narrow carbonation front width for the tested materials and exposure conditions. According to the Pourbaix diagram [20] for Fe-H_2O (10^{-6} mol/L), active corrosion starts at approx. pH 7 [21] for the OCP range measured. For this simplified system, therefore, active corrosion is not expected before thymolphthalein becomes colourless. The observations indicate that the width of the carbonation front may not have caused the early corrosion onset reported in the literature. However, cementitious materials do contain some chloride, and during carbonation the pH drops, which might increase the $[Cl^-]/[OH^-]$ ratio in the pore solution and thus the probability of corrosion.

4.3. Spatial variation of the carbonation depths in plain samples

For the plain tapped samples (C'), the carbonation depth on the top and lateral sides merged together is normally distributed (Figure 7). After 10 weeks of exposure, the average carbonation depth was 9.4 mm and the standard deviation of 0.7 mm. Assuming a cover depth of 10 mm and a reinforcement diameter of 6 mm, as used in the reinforced samples, the carbonation of the mortar embedding the steel would have been complete when the carbonation front had penetrated up to 16 mm. In Figure 12, the carbonation depth distribution in the plain mortar samples after 10 weeks of exposure is compared with the position of the reinforcement in the reinforced samples. After 10 weeks of exposure, 20% of the carbonation depth population in the plain mortar samples was higher than the cover (10 mm). Part of the steel was therefore embedded in carbonated mortar when the average value of the carbonation front was 9.4 mm. If we assume that the mortar is uniformly carbonated to a depth of 11.6 mm (worst-case scenario), 20% of the steel surface would be embedded in carbonated mortar. Considering the relationship between the carbonated fraction of mortar-steel interface and the OCP presented in Figure 11, positive OCP values are expected at this stage. Nevertheless, corrosion onset indicated by low potential values was observed for several of the rebars after 10 weeks (see Figures 3 and 4), which cannot be explained by the spatial distribution of the carbonation depth in the plain samples.

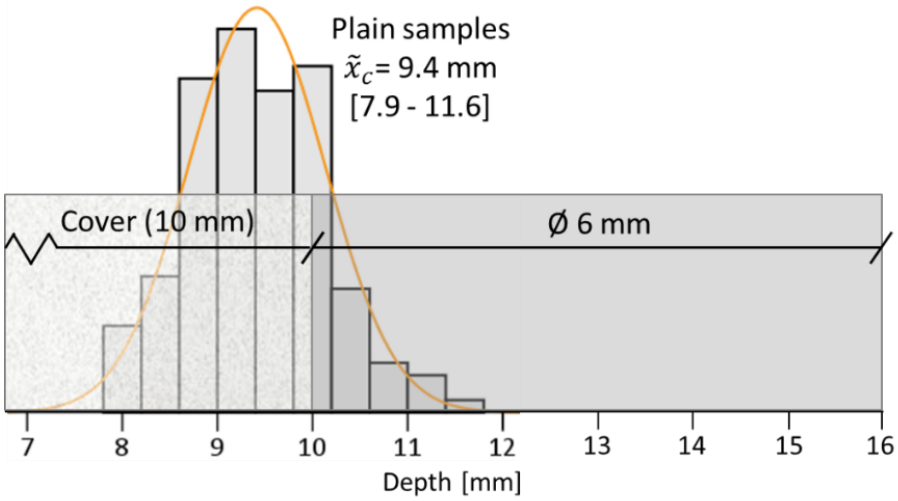

Figure 12: Comparison of the measured carbonation depth distribution in plain samples (type C') after 10 weeks (the lateral and top sides merged together) with the position of reinforcement in the reinforced samples. Note that the horizontal axis starts at 7 mm.

4.4. Spatial variation of the carbonation depth in reinforced samples

The observations made by Parrott [4], [5], Hussain et al. [6], and Yoon et al. [7], [8] were based on carbonation depth measured in plain samples. In the present investigation, we found that the presence of reinforcement has an impact on the spatial variation of the carbonation depth (cf. Figure 6). Figure 13 shows the carbonation depth distribution of the reinforced tapped (C-T) sample after 22 weeks of exposure. The carbonation depth was measured in areas without reinforcement ("M") and in the vicinity of the reinforcement ("R"). The data set includes the measurements from the top and lateral sides. The measurements are grouped in two populations: population "M", which is similar to the carbonation depth measured in the plain tapped (C-T) sample (Figure 7), and population "R", which presented higher carbonation depths. This shows that the reinforcement influenced the spatial variation of the carbonation depth distribution. The impact of embedded steel on carbonation development has also been observed by Köliö et al. [11], who report deeper carbonation depths in the vicinity of the reinforcement in cores extracted from façades exposed to natural carbonation.

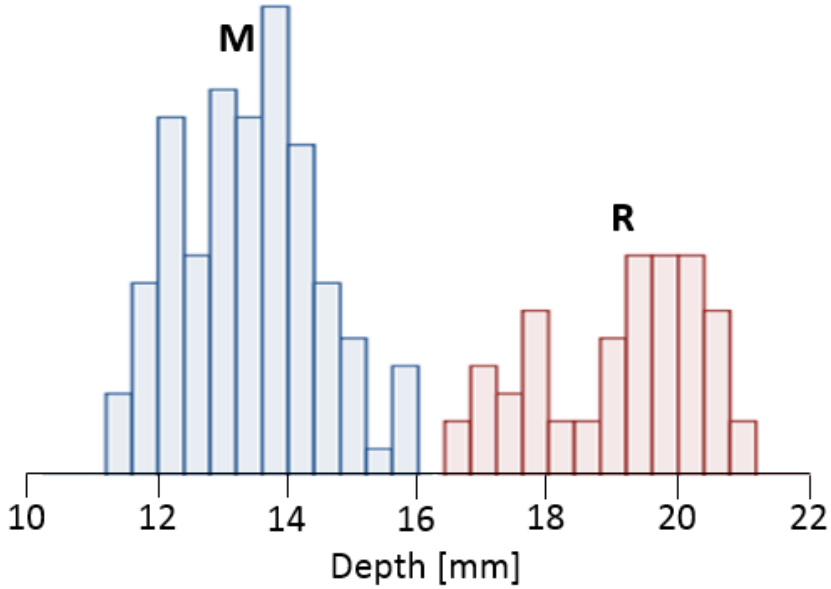

Figure 13: Carbonation depth distribution in C-T sample after 22 weeks of exposure. M: bulk mortar and R: vicinity of the reinforcement. Note that the horizontal axis starts at 10 mm.

A recent publication presented an overview of the characteristics of the concrete-steel interface [22]. One of the characteristics is the so-called ‘‘top-bar effect’’, which is defined as void formation under the horizontal rebars located mainly in the upper parts of the structural members as a result of segregation, settlement, and bleeding of fresh concrete [23]. This top-bar effect is observed to increase the higher in a cast section the position of the reinforcement is. Based on the shape of the carbonation front, which is evenly distributed around the top and middle reinforcements and the observation of micro-cracks radiating in all directions from the top and middle reinforcements (see Figure 10), we attribute the deeper carbonation depth in the vicinity of the reinforcement to these microstructural defects rather than to the top-bar effect. The assessment of the mortar-steel interface (see Figure 8 and Figure 9) indicated no bleeding underneath any of the rebars.

5. Conclusions

The aim of the present study was to investigate the conditions for carbonation-induced corrosion onset. In the literature, it has been observed that corrosion can initiate before the

apparent carbonation depth (measured in parallel plain samples) compares to the depth of the reinforcement. Plain and reinforced mortar samples were prepared. The samples were exposed to 20 °C, 60% RH and 1.5% CO_2 for up to 22 weeks. The open circuit potential (OCP) of the embedded steel was monitored and the carbonation development was followed by periodically spraying freshly split or dry-cut samples with thymolphthalein. The microstructure of the mortar around the rebars was investigated by optical microscopy on thin sections. The following conclusions can be drawn:

1. When plain and reinforced mortar samples are compared, corrosion onset is observed before the carbonation depth in the plain mortar samples compares to the cover depth of the reinforced samples. This apparent early corrosion onset is in agreement with the literature.
2. Neither the width of the carbonation front nor the spatial distribution of the carbonation depth in the plain samples can explain this apparent early corrosion onset.
3. However, the spatial variation of the carbonation depth was different in the reinforced and the plain mortar samples. Increased carbonation depth in the vicinity of the reinforcement was observed in the reinforced samples, which can explain the apparent early onset of corrosion reported in the literature.
4. Good agreement was observed between the carbonation of the mortar-steel interface and the corrosion potential drop. Corrosion does not start until the mortar-steel interface is (partially) carbonated.
5. When predicting carbonation-induced corrosion onset in field structures, the potential influence of reinforcement in carbonation development should be taken into account to avoid a non-conservative prediction.

Acknowledgements

The current paper is part of a larger research project, 'Lavkarbsem' (NFR project no. 235211/O30). The project is supported by the Norwegian Research Council and the following companies: Mapei AS, Norbetong AS, Norcem AS, Skanska AS, and Rambøll Engineering AS. The authors would also like to thank Marit Haugen (SINTEF) and Ulla Hjorth Jakobsen (DTI) for their assistance with the optical microscopy and Helga Synnøve Kjos-Hanssen and Elisabeth Leite Skare (NTNU) for their assistance in the laboratory.

References

1. Bamforth P (2004) Enhancing reinforced concrete durability: Guidance on selecting measures for minimising the risk of corrosion of reinforcement in concrete. Concrete Society Technical Report No. 61. Camberley, United Kingdom.

2. Bertolini L, Elsener B, Pedeferri P, Redaelli E, Polder R (2013) Chapter 5: Carbonation-induced corrosion. In: Corrosion of Steel in Concrete: Prevention, Diagnosis, Repair, 2nd edition. Wiley-VCH Verlag GmbH & Co, Weinheim, Germany, pp 79-92.

3. Anstice DJ, Page CL, Page MM (2005) The pore solution phase of carbonated cement pastes. Cement and Concrete Research 35 (2):377-383. doi:http://dx.doi.org/10.1016/j.cemconres.2004.06.041

4. Parrott LJ (1994) A study of carbonation-induced corrosion. Magazine of Concrete Research 46 (166):23-28. doi:doi:10.1680/macr.1994.46.166.23

5. Parrott LJ (1996) Some effects of cement and curing upon carbonation and reinforcement corrosion in concrete. Materials and Structures 29 (3):164-173. doi:10.1007/bf02486162

6. Yoon I-S, Çopuroğlu O, Park K-B (2007) Effect of global climatic change on carbonation progress of concrete. Atmospheric Environment 41 (34):7274-7285. doi:http://dx.doi.org/10.1016/j.atmosenv.2007.05.028

7. Hussain R, Ishida T (2009) Critical Carbonation Depth for Initiation of Steel corrosion in Fully Carbonated Concrete and Development of Electrochemical Carbonation Induced Corrosion Model. International Journal of Electrochemical Science 4 (8):1178-1195.

8. Hussain RR, Ishida T, Wasim M (2011) Experimental investigation of time dependent non-linear 3D relationship between critical carbonation depth and corrosion of steel in carbonated concrete. Corrosion Engineering, Science and Technology 46 (5):657-660. doi:10.1179/147842210X12659647007086

9. Japan Society of Civil Engineers (2007) Standard specifications for concrete structures: Design. JSCE Guidelines for Concrete No. 15.

10. Belda Revert A, De Weerdt K, Hornbostel K, Geiker MR (2016) Carbonation Characterization of Mortar with Portland Cement and Fly Ash, Comparison of Techniques Nordic Concrete Research 54 (1):60-76

11. Köliö A, Honkanen M, Lahdensivu J, Vippola M, Pentti M (2015) Corrosion products of carbonation induced corrosion in existing reinforced concrete facades. Cement and Concrete Research 78, Part B:200-207. doi:http://dx.doi.org/10.1016/j.cemconres.2015.07.009

12. EN-197-1 (2011) EN 197-1 Cement – Part 1: Composition, specifications and conformity criteria for common cements.

13. EN-196 (2005) EN 196-1:2005: Methods of testing cement – Part 1: Determination of strength.

14. NS-3576-3 (2012) NS-3576-3:2012. Armeringsstål. Mål og egenskaper. Del 3: Kamstål B500NC. (Steel for the reinforcement of concrete. Dimensions and properties. Part 3: Ribbed carbon steel B500NC).

15. EN-13295 (2003) EN 13295:2003: Products and systems for the protection and repair of concrete structures. Test methods. Determination of resistance to carbonation.

16. Norwegian Environment Agency (2015).

17. Nordtest (1999) Concrete, hardened: Water-cement ratio - NT Build 361.

18. RILEM TC 235-CTC Final test report on DTI's participation in round robin test (2014).

19. Belda Revert A, De Weerdt K, Geiker MR (2015) Carbonation front characterization pH colour indicators. 35th Cement and Concrete Science Conference, Aberdeen, Scotland.

20. Pourbaix M (1974). Atlas of Electrochemical Equilibria in Aqueous Solutions. Houston, USA, NACE International.

21. Küter A (2009). Management of Reinforcement Corrosion – A Thermodynamic Approach. PhD Thesis. Technical University of Denmark.

22. Angst UM, Geiker MR, Michel A, Gehlen C, Wong H, Isgor O B, Elsener B, Hansson CM, François R, Hornbostel K, Polder R, Alonso MC, Sanchez M, Correia MJ, Criado M, Sagüés A, Buenfeld N (2017) The steel–concrete interface. Materials and Structures 50 (2):143.

23. Zhang R, Castel A, François R (2011) Influence of steel–concrete interface defects owing to the top-bar effect on the chloride-induced corrosion of reinforcement. Magazine of Concrete Research 63 (10):773-81.